

# ADCK3, an Ancestral Kinase, Is Mutated in a Form of Recessive Ataxia Associated with Coenzyme Q<sub>10</sub> Deficiency

Clotilde Lagier-Tourenne,<sup>1</sup> Meriem Tazir,<sup>2</sup> Luis Carlos López,<sup>3</sup> Catarina M. Quinzii,<sup>3</sup> Mirna Assoum,<sup>1</sup> Nathalie Drouot,<sup>1</sup> Cleverson Busso,<sup>4</sup> Samira Makri,<sup>5</sup> Lamia Ali-Pacha,<sup>2</sup> Traki Benhassine,<sup>6</sup> Mathieu Anheim,<sup>1,7</sup> David R. Lynch,<sup>8</sup> Christelle Thibault,<sup>1</sup> Frédéric Plewniak,<sup>1</sup> Laurent Bianchetti,<sup>1</sup> Christine Tranchant,<sup>7</sup> Olivier Poch,<sup>1</sup> Salvatore DiMauro,<sup>3</sup> Jean-Louis Mandel,<sup>1</sup> Mario H. Barros,<sup>4</sup> Michio Hirano,<sup>3</sup> and Michel Koenig<sup>1,\*</sup>

Muscle coenzyme Q<sub>10</sub> (CoQ<sub>10</sub> or ubiquinone) deficiency has been identified in more than 20 patients with presumed autosomal-recessive ataxia. However, mutations in genes required for CoQ<sub>10</sub> biosynthetic pathway have been identified only in patients with infantile-onset multisystemic diseases or isolated nephropathy. Our SNP-based genome-wide scan in a large consanguineous family revealed a locus for autosomal-recessive ataxia at chromosome 1q41. The causative mutation is a homozygous splice-site mutation in the *aarF*-domain-containing kinase 3 gene (*ADCK3*). Five additional mutations in *ADCK3* were found in three patients with sporadic ataxia, including one known to have CoQ<sub>10</sub> deficiency in muscle. All of the patients have childhood-onset cerebellar ataxia with slow progression, and three of six have mildly elevated lactate levels. *ADCK3* is a mitochondrial protein homologous to the yeast *COQ8* and the bacterial *UbiB* proteins, which are required for CoQ biosynthesis. Three out of four patients tested showed a low endogenous pool of CoQ<sub>10</sub> in their fibroblasts or lymphoblasts, and two out of three patients showed impaired ubiquinone synthesis, strongly suggesting that *ADCK3* is also involved in CoQ<sub>10</sub> biosynthesis. The deleterious nature of the three identified missense changes was confirmed by the introduction of them at the corresponding positions of the yeast *COQ8* gene. Finally, a phylogenetic analysis shows that *ADCK3* belongs to the family of atypical kinases, which includes phosphoinositide and choline kinases, suggesting that *ADCK3* plays an indirect regulatory role in ubiquinone biosynthesis possibly as part of a feedback loop that regulates ATP production.

## Introduction

Recessive ataxias are a heterogeneous group of inherited neurodegenerative disorders that affect the cerebellum or the spinocerebellar and sensory tracts of the spinal cord. Several recessive ataxias, including Friedreich ataxia (FRDA [MIM 229300]), appear to be due to defective mitochondrial proteins. In FRDA and sideroblastic anemia/ataxia (ASAT [MIM 301310]), the defective proteins are involved in iron-sulfur cluster biogenesis, whereas in sensory ataxic neuropathy with dysarthria and ophthalmoparesis (SANDO [MIM 607459]) and in infantile-onset spinocerebellar ataxia (IOSCA [MIM 271245]), the defective proteins control mitochondrial DNA homeostasis.<sup>1–5</sup> In addition, recently reported forms of recessive ataxia are associated with muscle coenzyme Q<sub>10</sub> (CoQ<sub>10</sub>) deficiency<sup>6,7</sup> [MIM 607426] and might also involve genes encoding mitochondrial proteins because CoQ<sub>10</sub> is synthesized in mitochondria. CoQ<sub>10</sub> deficiency causes mitochondrial dysfunction because CoQ<sub>10</sub> carries electrons from complex I and complex II to complex III in the mitochondrial respiratory chain. Several forms of human coenzyme Q<sub>10</sub> deficiencies, all characterized by infantile encephalomyopathy, renal

failure, or both, have recently been attributed to mutations in specific CoQ<sub>10</sub> biosynthetic proteins (*COQ2*, *PDSS2*, and *PDSS1*).<sup>8–10</sup> Given that these were not null mutations, they should allow the production of either partially functional proteins or reduced levels of normal proteins, supporting the view that complete block of CoQ<sub>10</sub> synthesis would not be viable.

The genes involved in CoQ (ubiquinone) synthesis were identified by analysis of yeast and bacterial complementation groups of ubiquinone-deficient strains designated *coq1-coq10* and *ubiA-ubiH*, respectively. Most of them (*COQ* 1–3, *COQ* 5–7, *Ubi A*, *Ubi E–H*) correspond to specific enzymatic steps of ubiquinone synthesis.<sup>11,12</sup> Here, we describe the first recessive ataxia due to mutations in a *COQ8-UbiB* homolog, which most likely has an ancestral regulatory, rather than enzymatic, function.

## Material and Methods

### Subjects

We obtained clinical evaluation, blood samples, and skin biopsies after written informed consent as defined by the local ethics committees of the University Hospital of Algiers, Strasbourg, and the

<sup>1</sup>Institut de Génétique et de Biologie Moléculaire et Cellulaire, CNRS/INSERM/Université Louis Pasteur, et Collège de France, Chaire de génétique humaine, 67404 Illkirch, France; Hôpitaux Universitaires de Strasbourg, Strasbourg, F-67000 France; <sup>2</sup>Service de Neurologie, Centre Hospitalo-Universitaire Mustapha, Algiers 16000, Algeria; <sup>3</sup>Department of Neurology, Columbia University Medical Center, New York, NY 10032 USA; <sup>4</sup>Departamento de Microbiologia - ICB-II - Universidade de São Paulo, 05508-900, São Paulo, SP, Brasil; <sup>5</sup>Service de Neurologie, Hôpital Ait Idir, Algiers, Algeria; <sup>6</sup>Institut Pasteur d'Alger, El Hamma, Algiers, Algeria; <sup>7</sup>Service de Neurologie, Hôpitaux Universitaires de Strasbourg, 67091 Strasbourg, France; <sup>8</sup>Department of Neurology, University of Pennsylvania School of Medicine and Children's Hospital of Philadelphia, Philadelphia, PA 19104, USA

\*Correspondence: [mkoenig@igbmc.u-strasbg.fr](mailto:mkoenig@igbmc.u-strasbg.fr)

DOI 10.1016/j.ajhg.2007.12.024. ©2008 by The American Society of Human Genetics. All rights reserved.

Children's Hospital of Philadelphia. Affected individuals from family 1 were referred for autosomal recessive cerebellar ataxia, and DNA testing for Friedreich ataxia and AOA1 mutations was performed prior to linkage analysis. Primary fibroblasts from skin biopsies were obtained from patients 3, 5, and 6, and immortalized lymphoblastoid cell lines were obtained from patients 3, 5, and 7.

### Linkage Analysis

Genome-wide homozygosity mapping was performed with the GeneChip Human Mapping 10K 2.0 Xba Array from Affymetrix (Affymetrix, Santa Clara, CA). Sample processing and labeling were performed according to the manufacturer's instructions (Affymetrix Mapping 10K 2.0 Assay Manual, Version 1.0, 2004). Hybridization was performed with a GeneChip Hybridization oven 640, washed with the GeneChip Fluidics Station 450, and scanned with a GeneChip Scanner 3000. Single-nucleotide polymorphism (SNP) allele calls were generated by the GeneChip DNA Analysis Software version 3.0.2 (GDAS). Regions of homozygosity were defined by the presence of more than 25 consecutive homozygous SNPs and analyzed on HomoSNP software developed to visualize shared homozygous regions in consanguineous families (software available on request from [plewniak@igbmc.u-strasbg.fr](mailto:plewniak@igbmc.u-strasbg.fr)). The region of homozygosity by descent segregating with the disease was further analyzed with highly polymorphic microsatellite markers as described elsewhere.<sup>13</sup>

### Mutational Analysis

Mutational analysis was performed by PCR and direct sequencing of the 14 coding exons and the adjacent intronic junctions of human *ADCK3* gene (NM\_020247; primers and conditions available on request). PCR products were purified on Montage PCR<sub>96</sub> Cleanup Plates (Millipore, Bedford, MA) and used in sequencing reactions with the ABI BigDye Terminator Kit (Applied Biosystems), which were subsequently run on an ABI PRISM 3100 Genetic Analyzer. Computational analyses of mutations were carried out with Seqscape 2.5 software (Applied Biosystems). Parental segregation of the identified mutations was investigated in all available family members. *ADCK3* exon 8 and 11 splicing was analyzed by RT-PCR. Total RNA was extracted from primary fibroblasts or immortalized lymphoblastoid cells via Trizol according to the manufacturer's protocol (Invitrogen). Total RNA was reverse transcribed with the Superscript II kit (Invitrogen). PCR amplification was performed with primers located in exon 10 and exon 15 (forward 5'-CACCTGATTGACGTGCTGAG-3', reverse 5'-ATCTTC TCGGTGGTGCTCTG-3') and in exon 7 and exon 12 (forward 5'-CAACCCACCTGGCTAAG-3', reverse 5'-GGGGTCATAGAA GAAGTTGGA-3'). PCR products were separated on a 2% agarose gel and eluted with the Nucleospin extract II kit (Macherey-Nagel) before sequencing with the PCR forward and reverse primers.

### *ADCK4* mRNA Expression Analyses

#### by Quantitative RT-PCR

Relative expression levels of *ADCK4* mRNA were determined by real-time PCR with the LightCycler 480 protocol (Roche Biosciences) and a set of primers located in exon 13 and exon 15 (forward 5'-CGGGAGTTTGGGACAGAGT-3', reverse 5'-CCGACCCAA AGTCGTAAGG-3'). *ADCK4* mRNA expression was normalized to *β-actin* or to *RPLP0* mRNA expression. Data were analyzed with the  $2^{-\Delta\Delta Ct}$  method, and values are expressed as the mean of two separate experiments performed in duplicate.

### CoQ<sub>10</sub> Determination and CoQ<sub>10</sub> Biosynthesis Assay

Coenzyme Q<sub>10</sub> (CoQ<sub>10</sub>) in both fibroblasts and lymphoblasts ( $2-3 \times 10^6$  cells) was extracted in hexane and measured by high-performance liquid chromatography with electrochemical detection (HPLC-EQ).<sup>8,9</sup> An aliquot of the sample was used for protein determination with the BCA protein assay kit (Pierce). The results were expressed in ng of CoQ<sub>10</sub>/mg-protein. CoQ<sub>10</sub> biosynthesis in fibroblasts was measured by incorporation of labeled parahydroxybenzoate (<sup>14</sup>C-PHB) (450 Ci/mol).<sup>8,9</sup> After 48 hr of incubation with <sup>14</sup>C-PHB (0.02 mCi/ml) in the culture medium, radiolabeled CoQ<sub>10</sub> was extracted by hexane, isolated by HPLC with a C18 reverse-phase column, and collected and quantified in a scintillation counter. An aliquot of the sample was used for protein determination with the BCA protein assay kit (Pierce). The results were expressed in DPM/mg-protein/day.

### Respiratory-Chain Enzyme Activities

To measure the complex activities, fibroblasts were suspended in cold PBS ( $4-12 \times 10^6$  cells) and sonicated for 10 s to disrupt the membranes. An aliquot of the sample was used for protein determination with the BCA protein assay kit (Pierce). Complexes I and III (CI+III) activity was measured by observation of the reduction of cytochrome *c* (cyt *c*) at 550 nm.<sup>14</sup> In brief,  $4-12 \times 10^4$  cells were incubated at 30°C in a medium containing 10 mM KH<sub>2</sub>PO<sub>4</sub> (pH 7.8), 2 mM EDTA, 1 mg/ml BSA, 500 μM KCN, and 100 μM cyt *c*. After 2 min of incubation, the reaction was started by addition of 200 μM NADH, and the increase of absorbance is observed for an additional 2 min. The residual activity in the presence of rotenone (10 μg/ml) was subtracted from total activity. The results were expressed in nmol of reduced cyt *c*/min/mg-protein. Complex IV (or COX) activity was measured by observation of the reduction of cyt *c* at 550 nm.<sup>14</sup> In brief,  $8-24 \times 10^4$  cells were incubated at 30°C in a medium containing 10 mM KH<sub>2</sub>PO<sub>4</sub> (pH 6.5), 0.25 M sucrose, 1 mg/ml BSA, and 0.1% reduced cyt *c*, and the reaction was observed for 3 min. For inhibition of the reaction, 500 μM KCN was used. The results were expressed in nmol of oxidized cyt *c*/min/mg-protein. Citrate synthase (CS) activity was measured after the reduction of 100 μM 5,5'-dithiobis(2-nitrobenzoic acid) (DTNB) at 412 nm (30°C) in the presence of  $8-24 \times 10^4$  cells, 300 μM acetyl CoA, 10 mM Tris-Cl (pH = 7.5), and 500 μM oxaloacetic acid.<sup>14</sup> The results were expressed in nmol of TNB/min/mg-protein. The results of CI+III and COX activities were normalized to CS activity.

Complexes II and III activity was measured by observation of the reduction of cytochrome *c* at 550 nm.<sup>14</sup> In brief,  $4-12 \times 10^4$  cells were incubated at 30°C in medium containing 50 mM KH<sub>2</sub>PO<sub>4</sub>/K<sub>2</sub>HPO<sub>4</sub> (pH 7.5), 20 mM succinate, 1.5 mM KCN, and 2.5 μM rotenone KCN. After 10 min of incubation, the reaction was started by the addition of 50 μM cyt *c*, and increase of absorbance was observed for 2 min. The results were expressed in nmol of reduced cyt *c*/min/mg-protein and normalized to CS activity.

Complex III activity was measured by observation of the reduction of cytochrome *c* at 550 nm.<sup>14</sup> In brief,  $8-24 \times 10^4$  cells were incubated at 30°C in a medium containing 25 mM KH<sub>2</sub>PO<sub>4</sub> (pH 7.2), 5 mM MgCl<sub>2</sub>, 2.5 mg/ml BSA, 50 μg/ml Rotenone, and 15 μM reduced cyt *c*. After 3 min of incubation, the reaction was started by the addition of 350 μM ubiquinol, and the reaction was followed for 2 min. The results were expressed in nmol of oxidized cyt *c*/min/mg-protein and normalized to CS activity.

### Phylogenetic Tree and Multiple Alignment

The Uniprot protein-sequence database was searched with *ADCK3\_HUMAN* (647 residues) as a query, and a multiple

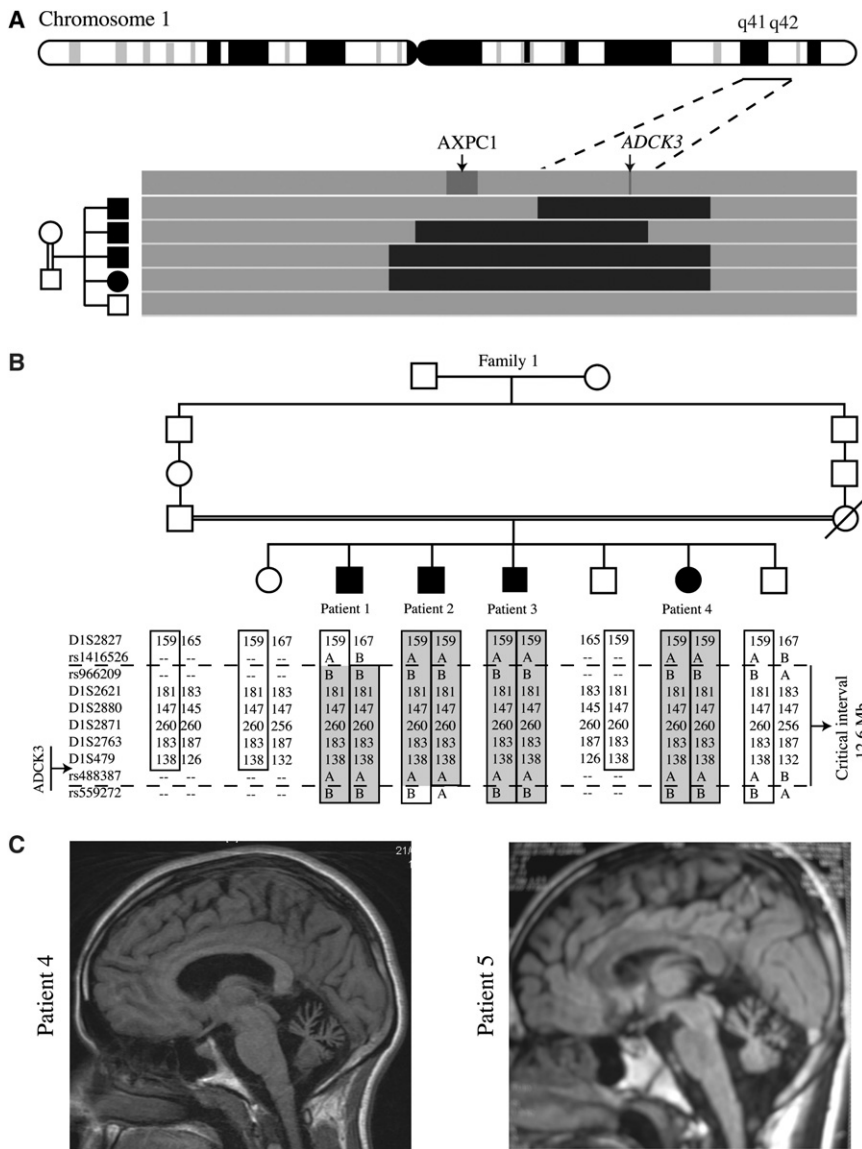


## Figure 1. Genotyping and Imaging Results of ARCA2 Families

(A) SNP results of family 1 for the chromosome 1q41-q42 region. Graphic interface (HomoSNP software) for visualization of shared regions of homozygosity in consanguineous families. The top horizontal bar indicates the position of recessive-ataxia loci and genes. Subsequent bars indicate individual results of the children represented on the left. The regions with more than 25 consecutive homozygous SNP are in black. The regions of heterozygosity are in gray. The four affected siblings in family 1 share a region of homozygosity by descent on chromosome 1q41-q42. The AXPC1 locus is centromeric to this region of homozygosity.

(B) Microsatellite analysis at chromosome 1q41-q42 in all available family 1 members. Markers are indicated on the left and are organized from top to bottom in the centromeric to telomeric order. Results of the four critical SNPs that define the two recombination boundaries are also indicated. Parental haplotypes linked with the disease are boxed. The region of homozygosity by descent is shaded in gray. Haplotype segregation confirms linkage between the 1q41-q42 locus and the disease in this family and defines a 12.6 Mb critical interval.

(C) Sagittal T1-weighted brain magnetic resonance imaging of patient 4 (family 1) and patient 5 (family 2) showing cerebellar atrophy and mild cerebral atrophy.

alignment of the detected homologous sequences was constructed with the PipeAlign tool.<sup>15</sup> A structural multiple alignment of the catalytic core domain of representative kinases has been previously proposed,<sup>16</sup> in which six atypical kinases and 25 protein kinases were aligned. For each of the six structurally aligned atypical kinase sequences, we downloaded from the PFAM<sup>17</sup> database seed alignments containing atypical kinase core domains, including 16 sequences of phosphatidylinositol phosphate kinase (PIPK) (PF01504), eight sequences of transient receptor potential (TRP) channel kinase domain (ChaK) (PF02816), 42 sequences of the phosphoinositide 3-kinase catalytic subunit (PI3K-PI4K) (PF00454), seven sequences of the actin-fragmin kinase (AFK) (PF09192), and 33 sequences of choline kinase (CKA-2) (PF01633). In addition, we downloaded a PFAM seed alignment of protein kinases (PF00069) containing 54 sequences. All collected seed alignments and the alignment obtained with ADCK3\_HUMAN as a query were concatenated and aligned on the basis of known protein-kinase motifs. The resulting multiple alignment of 221 sequences was manually refined in the SeqLab editor (Wisconsin package, Accelrys).

A phylogenetic tree was constructed with the neighbor-joining algorithm implemented in the phylowin program<sup>18</sup> from the

aligned sequences via the global gap-removal option and 500 bootstrap replicates. The iTOL tool<sup>19</sup> was used to generate the phylogenetic tree.

## Yeast Experiments

The *coq8* yeast point mutants were created by PCR with specific primers containing the related human mutations. These new yeast *coq8* alleles were then excised and cloned at the HindIII site of Yip352. These constructions were sequenced and the mutations confirmed. The recombinant plasmids were linearized with the internal NcoI site of *URA3*, and the linear fragment was used to transform the yeast strain W303DelCOQ8 by homologous recombination.<sup>20</sup> Purified individual transformants, the null mutant, and the wild-type W303-1A (Dr. R. Rothstein, Columbia University) were checked for growth on YPEG (1% yeast extract, 2% peptone, 2% ethanol, 3% glycerol, 2% agar) and YPD (1% yeast extract, 2% peptone, 2% glucose, 2% agar). Oxygen consumption and peroxide production were measured in yeast spheroplasts, isolated from cells grown on 2% galactose-rich media as described elsewhere.<sup>21</sup> Exogenous coenzyme Q<sub>6</sub> was added to a final concentration of 15  $\mu$ M in YPEG liquid media,<sup>22</sup> and growth was monitored by

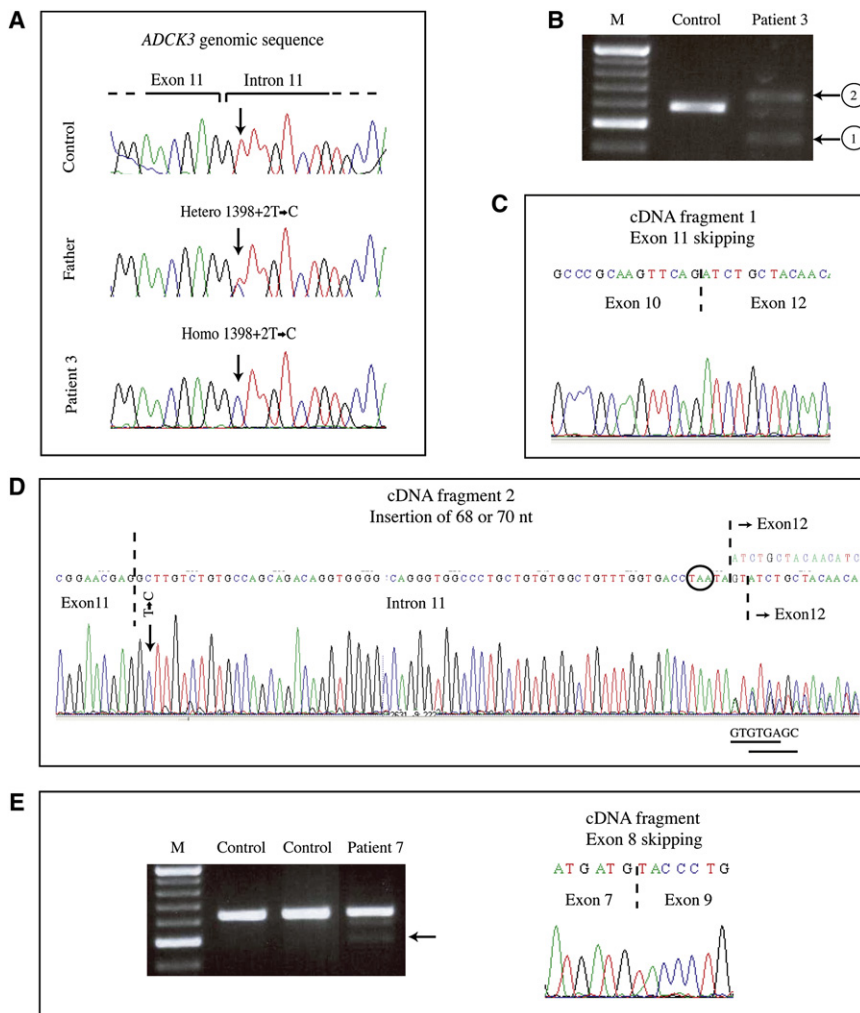


**Figure 2. Altered Splicing of *ADCK3* Exon 11 in Family 1 and Exon 8 in Family 4**  
 (A) Genomic sequence of *ADCK3* exon-intron 11 boundary of a control individual and of the father and patient 3 of family 1. The patient is homozygous for the donor splice-site mutation 1398+2T→C. The healthy father is heterozygous for this mutation.

(B) Analysis of RT-PCR products of patient 3 fibroblasts. The 1398+2T→C mutation affects exon 11 splicing and results in the production of two major bands on agarose gel, of 442 and 654 bp, respectively, and the product obtained from a control individual has a size of 584 bp. A faint band migrating between products 1 and 2 was shown by sequencing to correspond to heteroduplexes of products 1 and 2 (data not shown).

(C) Sequence of product 1 after elution from agarose gel. Product 1 corresponds to skipping of exon 11 leading to a frame-shift with a predicted truncated protein (p.Asp420TrpfsX40).

(D) Sequence of product 2 after elution from agarose gel. Product 2 corresponds to the use of two cryptic splice sites in intron 11 leading to the insertion of 68 and 70 nucleotides (nt), respectively. The sequence of the two alternative products is indicated above the chromatogram. The respective position of the two cryptic donor splice sites is indicated below the chromatogram (underlined). In both cases, 21 amino acids are inserted before an in frame stop codon (circled) leading to a predicted truncated protein (Ile467AlafsX22).

(E) Analysis of RT-PCR products of patient 7 lymphoblastoid cells. The c.993C→T mutation partially affects exon 8 splicing and results in the production of an abnormal product of 487 bp on agarose gel whereas only a normal product of 628 bp is seen in control lymphoblastoid cells. The abnormal product corresponds to skipping of exon 8 leading to an in-frame deletion of 47 amino acids (p.Lys314\_Gln360 del). The faint intermediate band was shown by sequencing to correspond to heteroduplexes (data not shown).

absorbance at 600 nm measurements for 10 days, at the end of which samples were taken and plated on YPD to check for possible contamination.

## Results

### *ADCK3* Mutations in ARCA2, a Novel Ataxia Syndrome

We performed linkage studies on a large consanguineous Algerian family with four individuals affected with childhood-onset cerebellar ataxia (family 1). We analyzed the four patients and one healthy sibling with 10K Affymetrix SNP arrays and identified, with a novel display program (Figure 1A), a unique region of homozygosity shared by all affected whereas the healthy sibling was heterozygous. The smallest region of overlap spanned 12.6 Mb on chromosome 1q41-q42 and did not overlap with the posterior

column ataxia and retinitis pigmentosa locus (AXPC1 [MIM 609033]),<sup>23</sup> located immediately centromeric (Figure 1A). The study of a dense set of microsatellite markers from the region in all available members of the family, including the father and two additional healthy siblings, confirmed linkage to the 1q41-42 locus (Figure 1B) with LOD-score calculation yielding a maximum 2-point value of 3.9 (theta = 0). Because four genes encoding mitochondrial proteins are already known to cause recessive ataxia when defective,<sup>1-4</sup> we prioritized sequencing of genes on the basis of the mitochondrial localization of their encoded products. We found a homozygous donor splice-site mutation (c.1398+2T→C, Figure 2A) in intron 11 of *ADCK3* (NM\_020247; aarF-domain-containing kinase 3; also known as *CABC1* [MIM 606980]) that was not present in 480 control chromosomes including 192 of North African origin. We carried out RT-PCR analysis

**Table 1. ADCK3 Mutations and Clinical Features in ARCA2 Patients**

	Family 1				Family 2	Family 3	Family 4
	Patient 1	Patient 2	Patient 3	Patient 4	Patient 5	Patient 6 <sup>a</sup>	Patient 7
Sex	M	M	M	F	M	M	F
Origin	Algeria	Algeria	Algeria	Algeria	Algeria	USA	France/Algeria
Mutation	Homo c.1398+2T→C	Homo c.1398+2T→C	Homo c.1398+2T→C	Homo c.1398+2T→C	Homo c.500_521 delinsTTG	Hetero c.[1541A→G] + [1750_1752 delACC]	Hetero c.[993C→ T] + [1645G→A]
Location	Intron 11	Intron 11	Intron 11	Intron 11	Exon 3	Exons 13 and 15	Exons 8 and 14
Predicted amino acid change	p.[Asp420Trp fsX40,Ile467 AlafsX22]	p.[Asp420Trp fsX40,Ile467 AlafsX22]	p.[Asp420Trp fsX40,Ile467 AlafsX22]	p.[Asp420Trp fsX40,Ile467 AlafsX22]	p.Gln167 LeufsX36	p.[Tyr514Cys] +[Thr584 del]	p.[Lys314_Gln360 del] + [Gly549Ser]
Age of onset	11	4	7	8	4	5	3
Disease duration	31	34	29	21	14	12	27
Cerebellar ataxia	+	+	+	+	+	+	+
Cerebellar atrophy	+	+	+	+	+	+	NA
Disability stage	3	3	3	3	3	3	3
Exercise intolerance	—	+	+	+	—	NA	NA
Reflexes	Absent ankle jerks	Normal	Brisk	Brisk	Normal	Brisk	Brisk
Hoffmann's sign	—	—	—	+	—	+	—
Babinski sign	—	—	—	—	—	—	—
Pes cavus	+	+	—	+	+	—	+
Mental retardation	—	Mild	—	—	Mild	—	Moderate (IQ: 54)
Lactic acidosis in mmol/l	NA	3.3 (n = 0.5–2.2)	2.9 (n = 0.5–2.2)	1.8–7.8 (n = 0.5–2.2)	1.29 (n = 0.5–2.2)	0.7 (n = 0.5–2.2)	0.98 (n = 1–1.7)
EMG	Normal	Normal	Normal	Normal	Mild axonal neuropathy	NA	Normal
Muscle biopsy	NA	NA	NA	NA	NA	Mild non specific changes	NA
Miscellaneous						Gynecomastia; feet and thumbs in dystonic position	Mild hearing loss

The following abbreviations are used: M, male; F = female; NA, not available; and EMG, electromyography. Disability stage grade 3: moderate, unable to run, limited walking without aid, in a scale from 0 (no signs or symptoms handicap) to 7 (bedridden).

<sup>a</sup> Patient 6 is individual 8 in reference <sup>6</sup>.

of *ADCK3* from fibroblast RNA of patient 3 and found three splice variants expressed from the mutant allele (Figures 2B–2D). In the shorter variant, exon 10 was skipped resulting in a frameshift (p.Asp420TrpfsX40) (Figure 2C). In the other variants, two cryptic splice sites in intron 11 were used, resulting in insertions of 68 and 70 nucleotides, with a stop codon after 21 residues (p.Ile467AlafsX22) (Figure 2D).

Three hundred and fifty-three families with non-Friedreich ataxia were analyzed either by homozygosity mapping at 1q41-q42 or by direct sequencing of *ADCK3* coding exons and flanking sequences. We identified five additional mutations (one single-amino-acid deletion, one truncating mutation, two missense mutations, and a predicted disruption of an SRp55 exonic splice enhancer) in three sporadic cases (Table 1). The three single-amino-acid changes affect conserved residues of the *ADCK3* protein (Figure 3) and were absent from 480 control chromosomes. Their pathogenicity was subsequently confirmed (see below). The nucleotide change in the predicted exonic

splice enhancer<sup>24,25</sup> in exon 8 was also absent from 480 control chromosomes, and its consequence was analyzed by RT-PCR from the patient's lymphoblastoid cell line. *ADCK3* transcript analysis revealed an abnormal product corresponding to skipping of exon 8 (Figure 2E) and leading to an in-frame deletion of 47 amino acids (p.Lys314\_Gln360 del).

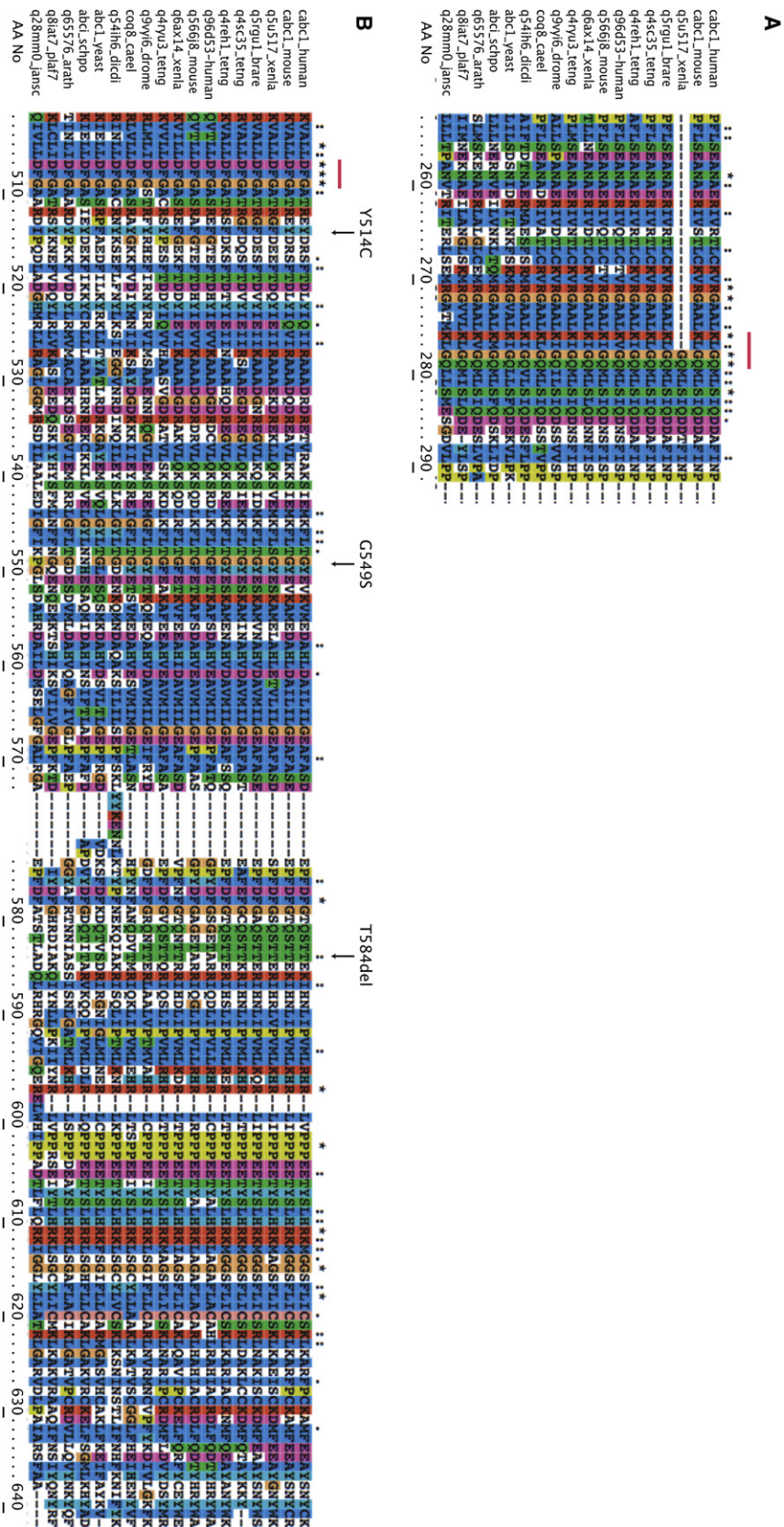
All affected individuals with mutations in *ADCK3* had childhood-onset gait ataxia and cerebellar atrophy (Figure 1C), with slow progression and few associated features (Table 1). Some patients had brisk tendon reflexes and Hoffmann's sign. Three patients had mild psychomotor retardation, and one patient had mild axonal degeneration of the sural nerve. None had renal dysfunction. Exercise intolerance and elevated serum lactate was present in three patients. Because cerebellar ataxia dominates the clinical presentation, we propose to name this entity ARCA2 (autosomal-recessive cerebellar ataxia 2), following the recent identification of ARCA1 [MIM 610743].<sup>26</sup>

**Figure 3. Conservation of Amino Acids Mutated in ARCA2 Patients among ADCK3–ADCK4 Protein Sequences**

SPTREMBL accession numbers are indicated on the left. *cabcl1\_human* and *q96d53\_human* correspond to ADCK3 and ADCK4, respectively. The following abbreviations are used: *Xenla*, *Xenopus laevis*; *brare*, *Brachydanio rerio*; *tetng*, *Tetraodon nigroviridis*; *drome*, *Drosophila melanogaster*; *caeel*, *Caenorhabditis elegans*; *dicdi*, *Dictyostelium discoideum*; *yeast*, *Saccharomyces cerevisiae*; *schpo*, *Schizosaccharomyces pombe*; *arath*, *Arabidopsis thaliana*; *plaf7*, *Plasmodium falciparum*; and *jansc*, *Jannaschia* sp. Amino acid numbering corresponds to human ADCK3. Dots and stars indicate variable degrees of phylogenetic conservation. Conserved amino acids are colored according to amino acid class (ClustalX). The N-terminal motif conserved in all members of the ADCK family (KxGK at positions 276–279) and the kinase motif VII (DFG at positions 507–509) are overlined in red. Nontruncating mutations identified in ARCA2 patients (p.Tyr514Cys, p.Gly549Ser, and p.Thr584 del) are indicated with arrows.

(A) ClustalX sequence alignments of ADCK3-specific N-terminal domain.  
 (B) ClustalX sequence alignments of ADCK3–ADCK4-specific C-terminal domain.

involved in coenzyme Q (ubiquinone) synthesis on the basis of yeast and bacterial complementation groups of ubiquinone-deficient strains.<sup>11,22</sup> Patient 6 was previously reported to have marked CoQ<sub>10</sub> deficiency in muscle (12.6 μg of CoQ<sub>10</sub>/g of fresh tissue; normal values 27.6 μg/g ± 4.4);<sup>6</sup> therefore, identification of ADCK3 mutations in this individual indicated that ADCK3 is also involved in CoQ synthesis in humans. To confirm this result in the absence of muscle biopsies from the other patients, we analyzed CoQ<sub>10</sub> levels and synthesis in cultured skin fibroblast or lymphoblastoid cell lines from patients 3, 5, 6, and 7 and found moderate but significant reduction in three (Table 2) and normal level in patient 3. In addition, because CoQ<sub>10</sub> is the electron carrier from respiratory complexes I and II to complex III, measuring of the combined activity of these enzymes assesses endogenous pools of CoQ<sub>10</sub> in mitochondria. These activities were significantly reduced in



**Coenzyme Q<sub>10</sub> Deficiency in ARCA2 Patients**  
 ADCK3 is a mitochondrial protein<sup>27</sup> that has yeast (ABC1/COQ8) and bacterial (UbiB) homologs known to be in-

**Table 2. Coenzyme Q<sub>10</sub> and Respiratory-Chain Enzyme Activities in ARCA2 Patients**

	Patient 3	Patient 5	Patient 6	Patient 7	Patient with <i>COQ2</i> Mutations <sup>a</sup>	Patient with <i>PDSS2</i> Mutations <sup>b</sup>	Controls
CoQ <sub>10</sub> levels in fibroblasts (ng/mg-protein)	69.0	<b>36.9</b> ± 6.5	<b>29.7</b>	NA	<b>24.8</b> ± 1.0	<b>13.0</b> ± 1.7	58.5 ± 4.1 n = 15
CoQ <sub>10</sub> levels in lymphoblasts (ng/mg-protein)	68.2	57.9 ± 13.9	NA	<b>48.5</b> ± 2.9	NA	NA	62.2 ± 2.8, n = 3
CoQ <sub>10</sub> biosynthesis assay in fibroblasts <sup>c</sup> (CoQ <sub>10</sub> DPM/mg-protein/day)	4108 ± 52	<b>2825</b>	<b>2006</b> ± 15	NA	<b>1349</b> ± 37	<b>789</b> ± 22	3569 ± 255, n = 5
CI+CIII/COX	<b>11.82</b>	<b>6.99</b>	<b>7.76</b>	NA	NA	NA	13.86 ± 1.27, n = 3
CI+CIII/CS	<b>6.36</b>	<b>3.70</b>	<b>4.13</b>	NA	NA	NA	8.03 ± 0.67, n = 3
CI+CIII/CS fold increase after addition of CoQ <sub>2</sub>	<b>1.88</b>	<b>2.15</b>	<b>2.47</b>	NA	NA	NA	1.26 ± 0.07, n = 3
CII+CIII/CS	0.46	<b>0.37</b>	<b>0.24</b>	NA	NA	NA	0.46 ± 0.02, n = 2
CIII/CS	0.65	0.83	0.62	NA	NA	NA	0.81 ± 0.18, n = 2

Abnormal values are shown in bold. When experiments were done more than once, values are given as means ± standard error of the mean. The following abbreviations are used: CI, complex I (NADH ubiquinone oxidoreductase); CII, complex II (succinate ubiquinone oxidoreductase); CIII, complex III (ubiquinol cytochrome c oxidoreductase); COX, cytochrome c oxidase; CS, citrate synthase; CoQ<sub>2</sub>, coenzyme Q<sub>2</sub> (strong rescue by CoQ<sub>2</sub> is indicative of CoQ deficiency); and DPM, decays per min.

<sup>a</sup> This patient with *COQ2* mutations was previously described.<sup>8</sup>

<sup>b</sup> This patient with *PDSS2* mutations was previously described.<sup>9</sup>

<sup>c</sup> By incorporation of <sup>14</sup>C-PHB (parahydroxybenzoate).

the fibroblasts of patients 5 and 6 and moderately reduced in those of patient 3. Moreover, addition of a short-chain quinone analog increased significantly complexes I+III activity in the fibroblasts of all patient tested, an indirect demonstration of CoQ<sub>10</sub> deficiency in these cells (Table 2). *ADCK3* mutations were therefore associated with CoQ<sub>10</sub> deficiency, although the defect was very mild in unaffected tissues of ARCA2 patients.

### ADCK3 Belongs to a Superfamily of Ancestral Protein and Nonprotein Kinases

ADCK proteins possess the conserved protein-kinase motifs<sup>28</sup> corresponding to regions required for ATP binding and for phosphotransfer reaction (the “universal core” consisting of motifs I, II, VIb, and VII) but do not conserve all of the usual kinase motifs (Figure 4A). In order to gain insights on the origin of the ADCK proteins, we analyzed the sequence of 61 prokaryotic and eukaryotic ADCK homologs and compared them to the sequence of 54 protein kinases and 106 atypical kinases. On the basis of the phylogenetic analysis of the “universal core” of the ADCK kinases (Figure 4B, and Figure S2 available online) and of the absence of the classical C-terminal motifs (Figure 4A), we propose that ADCKs belong to the so-called “atypical kinases” of the protein-kinase-like superfamily described by Scheeff and Bourne.<sup>16</sup> This superfamily comprises both nonprotein kinases, such as phosphoinositide and choline kinases, and atypical protein kinases, such as the actin-fragmin kinases (Figure 4B and Figure S2). The ADCK family comprises five paralogs in human (*ADCK1-5*). *ADCK3* and *ADCK4* are highly similar and appear to result from a gene duplication in vertebrates. In contrast, *ADCK1*, 2, and 5 have split from *ADCK3* and 4 very early during evolution because all eukaryotes and several, but not all, gram-negative bacteria possess at least one repre-

sentative of each subgroup (Figure S2). Yeast *ABC1/Coq8* is the ortholog of *ADCK3* and 4, whereas bacterial *UbiB* is more similar to the *ADCK1-ADCK5* subgroup. The “universal core” of ADCKs comprises a highly conserved lysine that binds the alpha phosphate and two highly conserved aspartates that bind the magnesium ions chelated by ATP. Interestingly, the p.Tyr514Cys mutation in patient 6 is located immediately after the second aspartate (DFG motif or motif VII, Figure 4A), strongly supporting a pathogenic effect of this amino acid change. The p.Gly549Ser is located outside the “universal core” but is highly conserved among members of the *ADCK3/ADCK4* subgroup (Figure 3), also supporting a pathogenic effect of the p.Gly549Ser change in patient 7. Gly549 is part of a C-terminal highly conserved segment, which is divergent not only from the classical protein-kinase domain, but also among the different subgroups of the ADCK family (Figure 4B and Figure S2), suggesting that proteins from each subgroup support a distinct function. On the other hand, all ADCK proteins share a common N-terminal domain (with invariable residues Lys276, Glu278, and Gln279; Figures 3 and 4A), which is absent from all other protein and nonprotein kinases and appears specifically related with ubiquinone metabolism.

### Nontruncating Mutations Introduced in the Yeast *ADCK3* Homolog Result in Impaired Respiration

For assessment of their pathogenicity, the three mutations resulting in single-amino-acid change (p.Tyr514Cys; p.Gly549Ser; and p.Thr584 del) were introduced on the yeast *coq8* mutant background. Yeast *coq* mutants grow on glucose but display impaired growth on nonfermentable carbon source (ethanol and glycerol), indicating a defect in respiration that can be rescued by exogenous CoQ<sub>6</sub> supplementation.<sup>22</sup> They produce high levels of H<sub>2</sub>O<sub>2</sub>

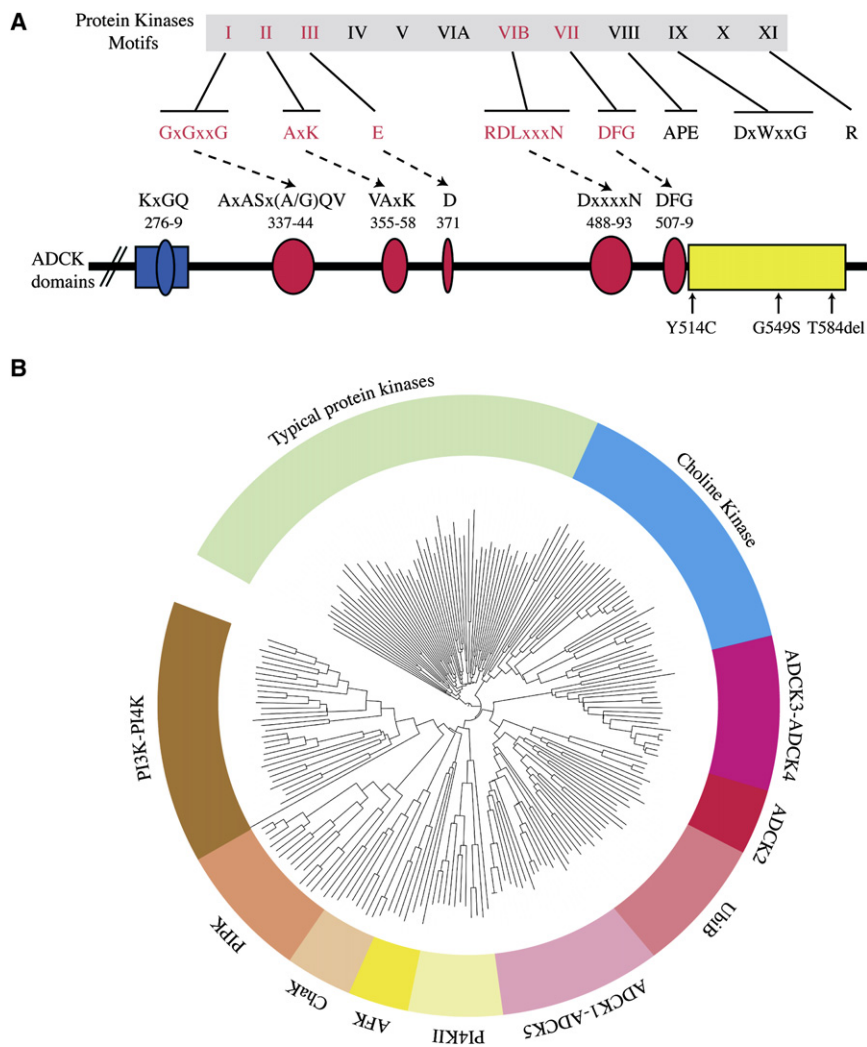


## Figure 4. Domain Organization and Phylogeny of ADCK Proteins

(A) Motif conservation in typical protein kinases and in ADCK proteins. Consensus of the eight most conserved motifs of the typical protein kinases are indicated on top. Motifs that share homology with ADCKs motifs are indicated in red. Consensus of ADCK motifs are indicated below, with amino acid positions corresponding to human ADCK3. ADCK domains are depicted on the diagram as follows: blue rectangle, N-terminal domain conserved among all members of the ADCK family and containing the KxGQ motif; red ovals, the position of the conserved kinase motifs; yellow rectangle, C-terminal domain specific for each ADCK subgroups. The position of single-amino-acid changes found in ARCA2 patients is indicated at the bottom. (B) Phylogenetic tree of typical and atypical protein kinases. Typical protein kinases are clustered in a single group. ADCK proteins are clustered in four groups. The UbiB group corresponds to the bacterial ADCKs and to the chloroplastic bacterial-like ADCKs. The following abbreviations are used: PI4KII, phosphatidylinositol 4 kinase type 2; AFK, actin-fragmin kinase; ChaK, TRP channel kinase; PIPK, Phosphatidylinositol Phosphate Kinase; and PI3K-PI4K, phosphatidylinositol 3 and 4 kinases and related protein kinases.

and display impaired oxygen consumption. The corresponding missense changes and single-amino-acid deletion (Phe372Cys, Gly407Ser, and Ser444del) were introduced into a yeast *COQ8* expression plasmid by site-directed mutagenesis. Transformation of yeast *Delcoq8* by mutant plasmids failed to restore growth on selective respiratory medium, whereas the wild-type sequence did, confirming the deleterious nature of the mutations (Figure 5A). Interestingly, replacement of Phe372 by the homologous human amino acid Tyr (corresponding to Tyr514) in the expression plasmid resulted in rescue when transfected in the *Delcoq8* mutant (Figure 5A), indicating that these two aromatic residues are interchangeable, a view also supported by their equal occurrence during evolution at this position (Figure 3). Moreover, oxygen consumption, H<sub>2</sub>O<sub>2</sub> production, and rescue by exogenous CoQ<sub>6</sub> were similar in *Delcoq8* mutants and *Delcoq8* yeast transformed with plasmids carrying the deleterious missense mutations (Figures 5B–5D). However, rescue by exogenous CoQ<sub>6</sub> was not as efficient in *coq8* mutants as in *coq7* or *coq2* mutants (Figure 5D), which are directly impaired in ubiquinone synthesis.

## Reduced Expression of the ADCK4 Paralog Correlates with CoQ<sub>10</sub> Deficiency in Fibroblasts

In order to test whether compensatory mechanisms regulate *ADCK4* expression in the case of *ADCK3* deficiency, we compared *ADCK4* mRNA expression by quantitative RT-PCR in three patient fibroblasts and in four control fibroblasts. *ADCK4* mRNA level was normal in patient 3 but, paradoxically, was mildly decreased in patients 5 and 6 (Figure 6). Because patient 3 fibroblasts had normal CoQ<sub>10</sub> levels and only moderately reduced complexes I+III activity compared to fibroblasts of patients 5 and 6 (Table 2), it appears that transcriptional downregulation of *ADCK4* parallels CoQ<sub>10</sub> levels in patient fibroblasts. The results suggest that *ADCK4*, the closest paralog of *ADCK3*, might also be involved in regulation of CoQ<sub>10</sub> synthesis. Further studies are needed to validate this observation and assess its relevance in affected tissues.

## Discussion

Familial cerebellar ataxia associated with muscle CoQ<sub>10</sub> deficiency was first reported in 2001.<sup>29</sup> Genes coding for



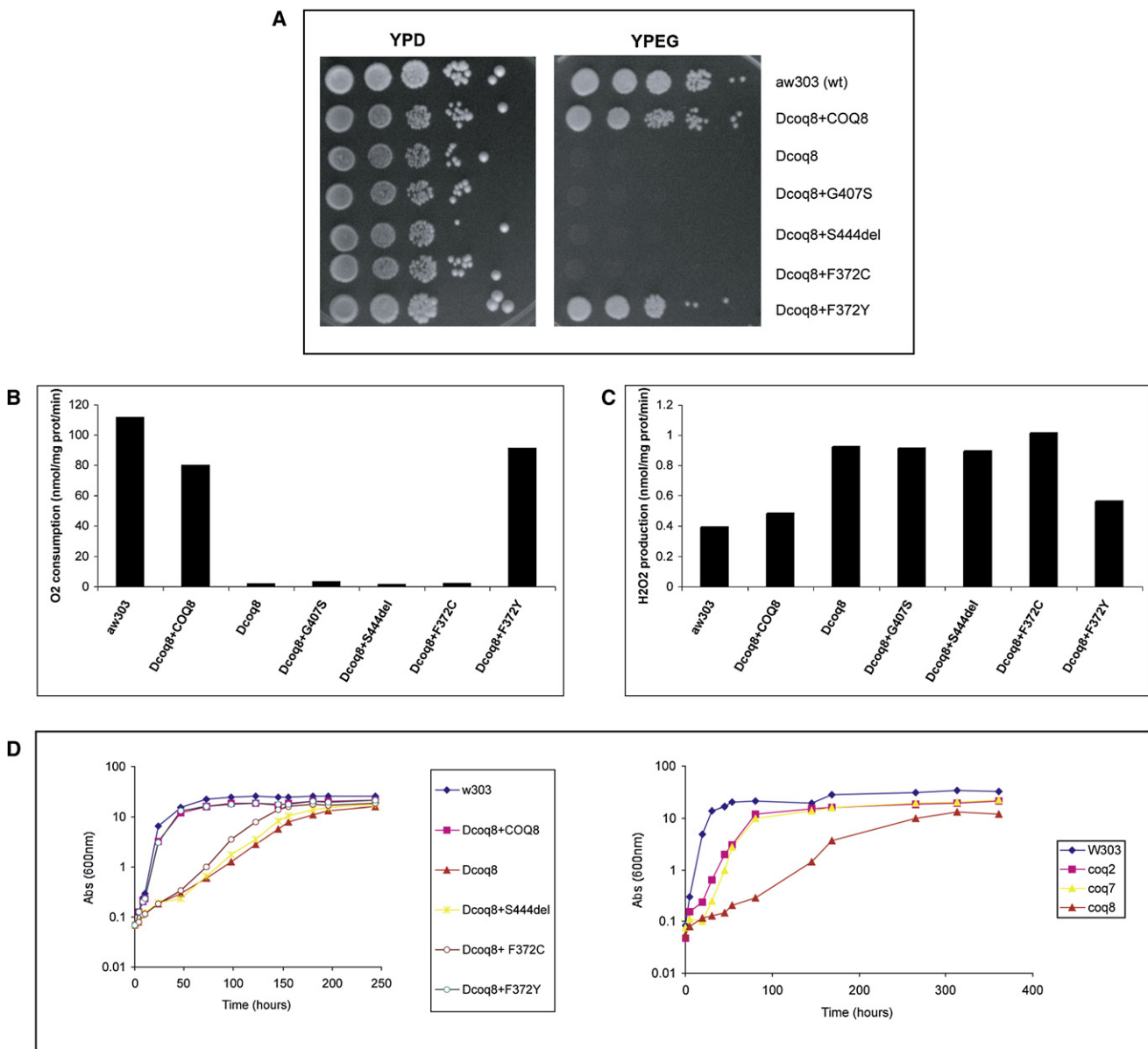


**Figure 5. *Coq8* Null Yeast Phenotype Was Not Rescued by Transfection with Plasmids Carrying the Nontruncating Mutations Identified in ARCA2 Patients**

(A) Serial dilutions of the wild-type AW303, the *coq8* null mutant (*Dcoq8* = *Delcoq8*), and the mutant transformed with yeast wild-type *COQ8* or with yeast *coq8* nontruncating mutations were spotted on rich glucose (YPD) and rich ethanol/glycerol (YPEG) plates. Growth on nonfermentable carbon source (YPEG) was not restored by mutant *coq8* but was rescued by the wild-type sequence and by the F372Y construct corresponding to the replacement of F372 by the homologous human amino acid (Y at the human position 514).

(B) Oxygen consumption is impaired in *coq8* null mutant (*Dcoq8*) and in *Dcoq8* yeast transformed with plasmids carrying the deleterious mutations.

(C) H<sub>2</sub>O<sub>2</sub> production is elevated in *coq8*-deficient strains. Impaired oxygen consumption and increased H<sub>2</sub>O<sub>2</sub> production are indicative of respiratory-chain dysfunction.

(D) Exogenous coenzyme Q (CoQ<sub>6</sub>) respiratory-growth rescue. Rescue was similar in *Dcoq8* strain and in *Dcoq8* yeast transformed with mutated plasmids and was less efficient than rescue of *coq7* and *coq2* yeast mutants.

enzymes involved in CoQ synthesis were candidates for this new form of ataxia. These genes have been identified by analysis of yeast and bacterial complementation groups of ubiquinone-deficient strains designated *coq1-coq10* and *ubiA-ubiH*, respectively; all have at least one homolog in humans, supporting the concept that CoQ

synthesis is a conserved pathway in all species. However, the first human mutations reported in genes encoding CoQ biosynthetic enzymes (PDSS1 and PDSS2, corresponding to COQ1 and COQ2, catalyze the first two specific steps of CoQ synthesis, and COQ2 catalyzes the second specific step) were identified in patients with severe

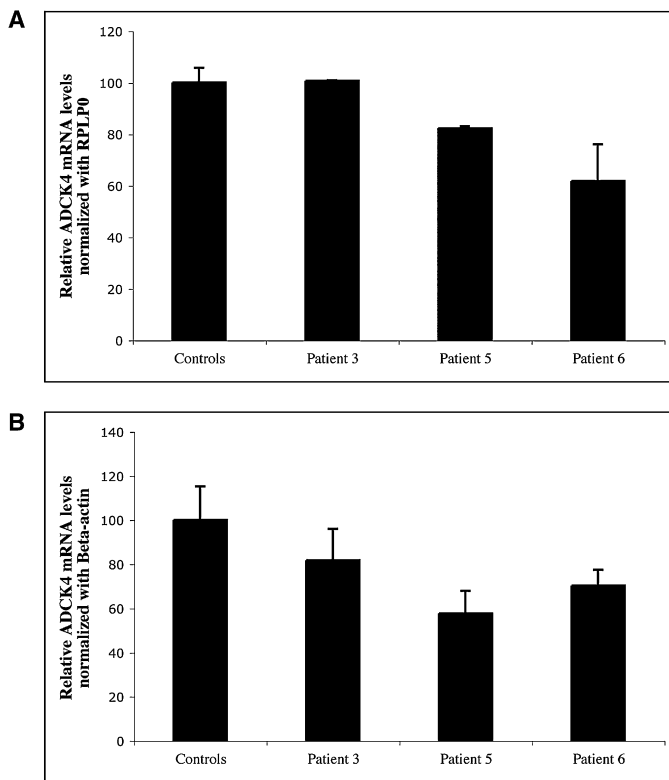


**Figure 6. Absence of ADCK4 Induction in ADCK3-Deficient Fibroblasts**

ADCK4 mRNA levels in control fibroblasts ( $n = 4$ ) and in patients 3, 5, and 6 fibroblasts were measured by quantitative real-time PCR. Expression levels of ADCK4 in patients 5 and 6 were slightly reduced. This slight reduction was not dependent on the type of housekeeping reference RNA used: (A) RPLP0 (ribosomal protein P0); (B)  $\beta$ -actin. Graphs represent means  $\pm$  standard deviation (SD) of two independent experiments performed in duplicates.

infantile-onset encephalomyopathy, renal failure, or both,<sup>8–10</sup> suggesting that direct impairment of CoQ<sub>10</sub> synthesis might not be associated with the milder forms of cerebellar ataxia. In fact, muscle CoQ<sub>10</sub> deficiency was found in some patients with ataxia with ocular apraxia type 1<sup>30</sup> (AOA1 [MIM 208920]), which thus became the first form of genetically defined ataxia to be associated with partial ubiquinone deficiency.<sup>31</sup> The relationship between aprataxin, the nuclear protein defective in AOA1, and muscle CoQ<sub>10</sub> deficiency is not known. To our knowledge, our identification of mutations in ADCK3, homologous to yeast COQ8 and to bacterial UbiB, documents for the first time that the defect of a mitochondrial protein involved in CoQ<sub>10</sub> synthesis can cause an almost pure form of autosomal-recessive cerebellar ataxia, which we named ARCA2. ARCA2 patients may be distinguished from other recessive ataxias by the presence of cerebellar atrophy with history of exercise intolerance in childhood and elevated serum lactate at rest or after moderate exercise. After excluding the index family, ARCA2 appears to be a rare cause of ataxia among European, U.S., and North African patients. The fact that we found ADCK3 mutations in a patient with previously reported muscle CoQ<sub>10</sub> deficiency<sup>6</sup> and the fact that other ARCA2 patients had moderate CoQ<sub>10</sub> deficiency in their fibroblast or lymphoblastoid cell lines suggest that ADCK3 is involved in CoQ synthesis, supporting the view that ADCK3, COQ8, and UbiB are functional homologs. CoQ<sub>10</sub> deficiency in ARCA2 patients raises the possibility of supplementation therapy. So far, only one patient (patient 6)<sup>6</sup> has been

treated with doses of CoQ<sub>10</sub> from 60 to 700 mg/day over 8 yr. The patient reported mild subjective improvement, and stabilization of the cerebellar ataxia was observed on examination. In three families, the identification of ADCK3 mutations was made solely on the basis of the ataxic phenotype and without knowledge of muscle CoQ<sub>10</sub> level, indicating that ARCA2 corresponds to a homogeneous syndrome, distinct from syndromes due to direct enzymatic block of CoQ<sub>10</sub> synthesis. The milder presentation of ARCA2 patients compared to patients with enzymatic block of CoQ<sub>10</sub> synthesis might be explained both by the redundancy of ADCK members in the human genome and by an indirect role of ADCK3 in CoQ<sub>10</sub> synthesis.

An indirect, regulatory role is supported by the similarity of the ADCKs with members of the superfamily of the atypical kinases. This finding leaves open the possibility that ADCK substrates might be protein or nonprotein molecules, making their identification an even more difficult task. The indirect role of ADCKs in CoQ synthesis is also supported by the delayed rescue by exogenous CoQ<sub>6</sub> of the yeast mutant strain *abc1/coq8*, compared to rescue of the *coq2* or *coq7* mutants, which are defective in *para*-hydroxybenzoate-polyprenyl transferase and 5-demethoxyubiquinol hydroxylase, respectively.<sup>32,33</sup> The delayed rescue of the *abc1/coq8* mutants compared to *coq2* or *coq7* mutants suggests that ABC1/COQ8 may also act downstream of CoQ production and may regulate additional pathways. Given the central role of CoQ in ATP synthesis, it is tempting to speculate that ADCKs regulate CoQ synthesis by phosphorylating substrates as part of a feedback loop that controls the level of ATP produced. In support of this hypothesis, it was observed that overexpression of ABC1/COQ8 has the ability to rescue other *coq* mutants. Indeed, overexpression of ABC1/COQ8 rescued the growth of *coq10* mutant by doubling the amount of mitochondrial coenzyme Q,<sup>34</sup> and it also suppressed a missense mutant of *coq9*.<sup>35</sup> Furthermore, in *coq* mutants there is global depletion of COQ3, COQ4, COQ6, COQ7, and COQ9, which appear to be part of a protein complex,<sup>20,36</sup> but not of COQ8, indicating that it is not part of the complex but affects its stability.<sup>36</sup> Despite the independent identification of aarF-domain-containing kinases (ADCKs) in 1998,<sup>28,37</sup> their substrates have remained elusive. The identification of mutations in

one ADCK member in cerebellar ataxia patients will certainly stimulate research on this family of ancestral kinases, in order to decipher the corresponding regulatory network and its relation with CoQ biosynthesis.

### Supplemental Data

Two figures can be found with this article online at <http://www.ajhg.org/>.

### Acknowledgments

We are indebted to H. Puccio, S. Schmucker, L. Reutenauer, C. Grussenmeyer, S. Didaoui, and Adolfo T. Barbosa for advice and technical help. We wish to thank D. H'mida for support and fruitful discussions, A. Mota and E.G. Nobrega (Genomas UNIVAP laboratory) for technical help, S. Vicaire and I. Colas for DNA sequencing, B. Heller (IGBMC) and I. Bezier (Genethon, Evry) for cell-culture assistance, and Catherine Clarke (University of California) for yeast strains. This study was supported by funds from the Agence Nationale pour la Recherche-Maladies Rares (ANR-MRAR) to M.K; the Institut National de la Santé et de la Recherche Médicale, the Centre National de la Recherche Scientifique, and the Collège de France (J.-L.M.); the FAPESP (M.H.B); National Institutes of Health grants NS11766 and HD32062 (M.H); the Ministerio de Educación y Ciencia from Spain (L.C.L); and the Muscle Dystrophy Association (C.M.Q).

Received: October 19, 2007

Revised: December 15, 2007

Accepted: December 28, 2007

Published online: March 6, 2008

### Web Resources

The URLs for data presented herein are as follows:

Ensembl Genome Browser, <http://www.ensembl.org/index.html>  
Exonic splicing enhancers Finder (ESEFinder), <http://rulai.cshl.edu/cgi-bin/tools/ESE3/esefinder.cgi?process=home>  
Genebank, <http://www.ncbi.nlm.nih.gov/Genbank/>  
Interactive Tree of Life (ITOL), <http://itol.embl.de/index.shtml>  
Online Mendelian Inheritance in Man (OMIM), <http://www.ncbi.nlm.nih.gov/Omim/>  
UCSC Genome Browser, <http://www.genome.ucsc.edu>

### References

1. Campuzano, V., Montermini, L., Molto, M.D., Pianese, L., Cossee, M., Cavalcanti, F., Monros, E., Rodius, F., Duclos, F., Monticelli, A., et al. (1996). Friedreich's ataxia: Autosomal recessive disease caused by an intronic GAA triplet repeat expansion. *Science* 271, 1423–1427.
2. Allikmets, R., Raskind, W.H., Hutchinson, A., Schueck, N.D., Dean, M., and Koeller, D.M. (1999). Mutation of a putative mitochondrial iron transporter gene (ABC7) in X-linked sideroblastic anemia and ataxia (XLSA/A). *Hum. Mol. Genet.* 8, 743–749.
3. Nikali, K., Suomalainen, A., Saharinen, J., Kuokkanen, M., Spelbrink, J.N., Lonnqvist, T., and Peltonen, L. (2005). Infantile onset spinocerebellar ataxia is caused by recessive mutations in mitochondrial proteins Twinkle and Twinky. *Hum. Mol. Genet.* 14, 2981–2990.
4. Van Goethem, G., Martin, J.J., Dermaut, B., Lofgren, A., Wibail, A., Ververken, D., Tack, P., Dehaene, I., Van Zandijcke, M., Moonen, M., et al. (2003). Recessive POLG mutations presenting with sensory and ataxic neuropathy in compound heterozygote patients with progressive external ophthalmoplegia. *Neuromuscul. Disord.* 13, 133–142.
5. Winterthun, S., Ferrari, G., He, L., Taylor, R.W., Zeviani, M., Turnbull, D.M., Engelsens, B.A., Moen, G., and Bindoff, L.A. (2005). Autosomal recessive mitochondrial ataxic syndrome due to mitochondrial polymerase gamma mutations. *Neurology* 64, 1204–1208.
6. Lamperti, C., Naini, A., Hirano, M., De Vivo, D.C., Bertini, E., Servidei, S., Valeriani, M., Lynch, D., Banwell, B., Berg, M., et al. (2003). Cerebellar ataxia and coenzyme Q10 deficiency. *Neurology* 60, 1206–1208.
7. Aure, K., Benoist, J.F., Ogier de Baulny, H., Romero, N.B., Rigal, O., and Lombs, A. (2004). Progression despite replacement of a myopathic form of coenzyme Q10 defect. *Neurology* 63, 727–729.
8. Quinzii, C., Naini, A., Salviati, L., Trevisson, E., Navas, P., Dimauro, S., and Hirano, M. (2006). A mutation in para-hydroxybenzoate-polypropenyl transferase (COQ2) causes primary coenzyme Q10 deficiency. *Am. J. Hum. Genet.* 78, 345–349.
9. Lopez, L.C., Schuelke, M., Quinzii, C.M., Kanki, T., Rodenburg, R.J., Naini, A., Dimauro, S., and Hirano, M. (2006). Leigh syndrome with nephropathy and CoQ10 deficiency due to decaprenyl diphosphate synthase subunit 2 (PDSS2) mutations. *Am. J. Hum. Genet.* 79, 1125–1129.
10. Mollet, J., Giurgea, I., Schlemmer, D., Dallner, G., Chretien, D., Delahodde, A., Bacq, D., de Lonlay, P., Munnich, A., and Rotig, A. (2007). Prenyldiphosphate synthase, subunit 1 (PDSS1) and OH-benzoate polypropenyltransferase (COQ2) mutations in ubiquinone deficiency and oxidative phosphorylation disorders. *J. Clin. Invest.* 117, 765–772.
11. Poon, W.W., Davis, D.E., Ha, H.T., Jonassen, T., Rather, P.N., and Clarke, C.F. (2000). Identification of Escherichia coli ubiB, a gene required for the first monooxygenase step in ubiquinone biosynthesis. *J. Bacteriol.* 182, 5139–5146.
12. Tran, U.C., and Clarke, C.F. (2007). Endogenous synthesis of coenzyme Q in eukaryotes. *Mitochondrion Suppl.* 7, S62–S71.
13. Lagier-Tourenne, C., Tranebjaerg, L., Chaigne, D., Gribaa, M., Dollfus, H., Silvestri, G., Betard, C., Warter, J.M., and Koenig, M. (2003). Homozygosity mapping of Marinesco-Sjogren syndrome to 5q31. *Eur. J. Hum. Genet.* 11, 770–778.
14. Barrientos, A. (2002). In vivo and in organello assessment of OXPHOS activities. *Methods* 26, 307–316.
15. Plewniak, F., Bianchetti, L., Breilvet, Y., Carles, A., Chalmel, F., Lecompte, O., Mochel, T., Moulinier, L., Muller, A., Muller, J., et al. (2003). PipeAlign: A new toolkit for protein family analysis. *Nucleic Acids Res.* 31, 3829–3832.
16. Scheeff, E.D., and Bourne, P.E. (2005). Structural evolution of the protein kinase-like superfamily. *PLoS Comput Biol* 1, e49.
17. Finn, R.D., Mistry, J., Schuster-Bockler, B., Griffiths-Jones, S., Hollich, V., Lassmann, T., Moxon, S., Marshall, M., Khanna, A., Durbin, R., et al. (2006). Pfam: Clans, web tools and services. *Nucleic Acids Res.* 34, D247–D251.
18. Galtier, N., Gouy, M., and Gautier, C. (1996). SEAVIEW and PHYLO\_WIN: Two graphic tools for sequence alignment and molecular phylogeny. *Comput. Appl. Biosci.* 12, 543–548.

19. Letunic, I., and Bork, P. (2007). Interactive Tree Of Life (iTOL): An online tool for phylogenetic tree display and annotation. *Bioinformatics* 23, 127–128.
20. Hsu, A.Y., Do, T.Q., Lee, P.T., and Clarke, C.F. (2000). Genetic evidence for a multi-subunit complex in the O-methyltransferase steps of coenzyme Q biosynthesis. *Biochim. Biophys. Acta* 1484, 287–297.
21. Tahara, E.B., Barros, M.H., Oliveira, G.A., Netto, L.E., and Kowaltowski, A.J. (2007). Dihydrolipoyl dehydrogenase as a source of reactive oxygen species inhibited by caloric restriction and involved in *Saccharomyces cerevisiae* aging. *FASEB J.* 21, 274–283.
22. Do, T.Q., Hsu, A.Y., Jonassen, T., Lee, P.T., and Clarke, C.F. (2001). A defect in coenzyme Q biosynthesis is responsible for the respiratory deficiency in *Saccharomyces cerevisiae* abc1 mutants. *J. Biol. Chem.* 276, 18161–18168.
23. Higgins, J.J., Morton, D.H., and Loveless, J.M. (1999). Posterior column ataxia with retinitis pigmentosa (AXPC1) maps to chromosome 1q31-q32. *Neurology* 52, 146–150.
24. Cartegni, L., Wang, J., Zhu, Z., Zhang, M.Q., and Krainer, A.R. (2003). ESEfinder: A web resource to identify exonic splicing enhancers. *Nucleic Acids Res.* 31, 3568–3571.
25. Smith, P.J., Zhang, C., Wang, J., Chew, S.L., Zhang, M.Q., and Krainer, A.R. (2006). An increased specificity score matrix for the prediction of SF2/ASF-specific exonic splicing enhancers. *Hum. Mol. Genet.* 15, 2490–2508.
26. Gros-Louis, F., Dupre, N., Dion, P., Fox, M.A., Laurent, S., Verreault, S., Sanes, J.R., Bouchard, J.P., and Rouleau, G.A. (2007). Mutations in SYNE1 lead to a newly discovered form of autosomal recessive cerebellar ataxia. *Nat. Genet.* 39, 80–85.
27. Iizumi, M., Arakawa, H., Mori, T., Ando, A., and Nakamura, Y. (2002). Isolation of a novel gene, CABC1, encoding a mitochondrial protein that is highly homologous to yeast activity of bc1 complex. *Cancer Res.* 62, 1246–1250.
28. Leonard, C.J., Aravind, L., and Koonin, E.V. (1998). Novel families of putative protein kinases in bacteria and archaea: Evolution of the “eukaryotic” protein kinase superfamily. *Genome Res.* 8, 1038–1047.
29. Musumeci, O., Naini, A., Slonim, A.E., Skavin, N., Hadjigeorgiou, G.L., Krawiecki, N., Weissman, B.M., Tsao, C.Y., Mendell, J.R., Shanske, S., et al. (2001). Familial cerebellar ataxia with muscle coenzyme Q10 deficiency. *Neurology* 56, 849–855.
30. Le Ber, I., Dubourg, O., Benoist, J.F., Jardel, C., Mochel, F., Koenig, M., Brice, A., Lombes, A., and Durr, A. (2007). Muscle coenzyme Q10 deficiencies in ataxia with oculomotor apraxia 1. *Neurology* 68, 295–297.
31. Quinzii, C.M., Kattah, A.G., Naini, A., Akman, H.O., Mootha, V.K., DiMauro, S., and Hirano, M. (2005). Coenzyme Q deficiency and cerebellar ataxia associated with an aprataxin mutation. *Neurology* 64, 539–541.
32. Ashby, M.N., Kutsunai, S.Y., Ackerman, S., Tzagoloff, A., and Edwards, P.A. (1992). COQ2 is a candidate for the structural gene encoding para-hydroxybenzoate:polyprenyltransferase. *J. Biol. Chem.* 267, 4128–4136.
33. Marbois, B.N., and Clarke, C.F. (1996). The COQ7 gene encodes a protein in *saccharomyces cerevisiae* necessary for ubiquinone biosynthesis. *J. Biol. Chem.* 271, 2995–3004.
34. Barros, M.H., Johnson, A., Gin, P., Marbois, B.N., Clarke, C.F., and Tzagoloff, A. (2005). The *Saccharomyces cerevisiae* COQ10 gene encodes a START domain protein required for function of coenzyme Q in respiration. *J. Biol. Chem.* 280, 42627–42635.
35. Johnson, A., Gin, P., Marbois, B.N., Hsieh, E.J., Wu, M., Barros, M.H., Clarke, C.F., and Tzagoloff, A. (2005). COQ9, a new gene required for the biosynthesis of coenzyme Q in *Saccharomyces cerevisiae*. *J. Biol. Chem.* 280, 31397–31404.
36. Hsieh, E.J., Gin, P., Gulmezian, M., Tran, U.C., Saiki, R., Marbois, B.N., and Clarke, C.F. (2007). *Saccharomyces cerevisiae* Coq9 polypeptide is a subunit of the mitochondrial coenzyme Q biosynthetic complex. *Arch. Biochem. Biophys.* 463, 19–26.
37. Macinga, D.R., Cook, G.M., Poole, R.K., and Rather, P.N. (1998). Identification and characterization of aarF, a locus required for production of ubiquinone in *Providencia stuartii* and *Escherichia coli* and for expression of 2'-N-acetyltransferase in *P. stuartii*. *J. Bacteriol.* 180, 128–135.